Citation: Molecular Therapy–Nucleic Acids (2013) 2, e92; doi:10.1038/mtna.2013.24

www.nature.com/mtna

U1 Adaptor Oligonucleotides Targeting *BCL2* and *GRM1* Suppress Growth of Human Melanoma Xenografts *In Vivo*

Rafal Goraczniak[1], Brian A Wall[2], Mark A Behlke[3], Kim A Lennox[3], Eric S Ho[4], Nikolas H Zaphiros[4], Christopher Jakubowski[4], Neil R Patel[4], Steven Zhao[4], Carlo Magaway[4], Stacey A Subbie[4], Lumeng Jenny Yu[2], Stephanie LaCava[2], Kenneth R Reuhl[5], Suzie Chen[2], and Samuel I Gunderson[4]

U1 Adaptor is a recently discovered oligonucleotide-based gene-silencing technology with a unique mechanism of action that targets nuclear pre-mRNA processing. U1 Adaptors have two distinct functional domains, both of which must be present on the same oligonucleotide to exert their gene-silencing function. Here, we present the first *in vivo* use of U1 Adaptors by targeting two different human genes implicated in melanomagenesis, B-cell lymphoma 2 (*BCL2*) and metabotropic glutamate receptor 1 (*GRM1*), in a human melanoma cell xenograft mouse model system. Using a newly developed dendrimer delivery system, anti-*BCL2* U1 Adaptors were very potent and suppressed tumor growth at doses as low as 34 µg/kg with twice weekly intravenous (iv) administration. Anti-*GRM1* U1 Adaptors suppressed tumor xenograft growth with similar potency. Mechanism of action was demonstrated by showing target gene suppression in tumors and by observing that negative control U1 Adaptors with just one functional domain show no tumor suppression activity. The anti-*BCL2* and anti-*GRM1* treatments were equally effective against cell lines harboring either wild-type or a mutant V600E B-RAF allele, the most common mutation in melanoma. Treatment of normal immune-competent mice (C57BL6) indicated no organ toxicity or immune stimulation. These proof-of-concept studies represent an in-depth (over 800 mice in ~108 treatment groups) validation that U1 Adaptors are a highly potent gene-silencing therapeutic and open the way for their further development to treat other human diseases.

Molecular Therapy–Nucleic Acids (2013) **2**, e92; doi:10.1038/mtna.2013.24; published online 14 May 2013
Subject Category: Antisense Oligonucleotides; Therapeutic Proof-of-Concept

Introduction

The ability to silence a single target gene with minimal toxicity and few off-target effects (OTEs) would offer the medical community new tools to combat a wide variety of diseases. Several hybridization-based technologies have been tested over the past 30 years that utilize synthetic oligonucleotides to suppress expression of a specific target gene. In broad terms, these technologies are based on a gene being targeted either by small interfering RNAs (siRNAs) which exploit the natural cellular RNA interference machinery[1,2] or by an antisense oligonucleotide (ASO) that can function *via* a variety of mechanisms, including RNase H-mediated cleavage of RNA, steric hindrance of mRNA translation, splice site switching, and miRNA antagonists.[3–5] ASOs and siRNAs have struggled to produce commercially viable therapeutics, in spite of initial excitement and large-scale investment[6] presenting an opportunity for alternative gene-silencing technologies.

U1 Adaptors are a recently invented gene-silencing technology that exploits the natural ability of the U1 small nuclear ribonucleoprotein (snRNP) splicing factor to inhibit gene-specific polyA site activity of the target gene, a regulated nuclear pre-mRNA processing step obligatory for nearly all RNA Polymerase II genes.[7–12] A U1 Adaptor is a synthetic oligonucleotide (typically 28–33 nucleotides) comprised of a 5′ target domain (TD), which binds to the target pre-mRNA, and a 3′ U1 domain (U1D), which binds to the 5′-end of the U1 small nuclear RNA subunit of U1 snRNP.[7,8] Tethering of the U1 snRNP to a target pre-mRNA blocks maturation leading to reduced levels of mature mRNA. The U1D sequence is common to all U1 Adaptors and is defined by the U1 snRNP; design and chemical modification patterns have already been optimized.[7] In contrast, the TD sequence is target-specific and hence unique to each U1 Adaptor. Like all other gene knockdown technologies, empiric testing is required for site selection and optimization. Extensive medicinal chemistry studies have been done in ASO and siRNA systems to find chemical modifications that improve nuclease stability, enhance potency, and reduce OTEs.[3,5,13–17] Unlike siRNAs or RNase H-mediated ASOs, U1 Adaptors do not interact or function with any cellular enzymes (such as RNase H, Dicer, Argonaut 2, etc.) and thus can be made entirely using modified components, such as 2′-O-Methyl RNA (2′OMe) or locked nucleic acids (LNAs), with or without phosphorothioate (PS)-modified internucleotide linkages.[7] All oligonucleotide-based silencing technologies have associated toxicities and U1 Adaptors are no exception, as evidenced by a recent report that showed significant OTEs when used at high doses.[18] In a previous report, use of U1 Adaptors at a lower dose gave effective and specific silencing with few OTEs.[7]

Here, we present the first report of *in vivo* use of U1 Adaptors by targeting two human genes to suppress growth of human melanoma cells in a mouse xenograft model system.

[1]Silagene Inc., Hillsborough, New Jersey, USA; [2]Department of Chemical Biology, Rutgers University, Ernest Mario School of Pharmacy, Piscataway, New Jersey, USA; [3]Integrated DNA Technologies Inc., Coralville, Iowa, USA; [4]Department of Molecular Biology and Biochemistry, Rutgers University, Piscataway, New Jersey, USA; [5]Department of Pharmacology and Toxicology, Rutgers University, Ernest Mario School of Pharmacy, Piscataway, New Jersey, USA. Correspondence: Samuel I Gunderson, Department of Molecular Biology and Biochemistry, Rutgers University, 604 Allison Rd Room A322, Piscataway, New Jersey 08854, USA. E-mail: gunderson@biology.rutgers.edu or Mark A Behlke, Integrated DNA Technologies Inc., 1710 Commercial Park, Coralville, Iowa 52241, USA. E-mail: mbehlke@idtdna.com
Keywords: cancer therapy; dendrimer; gene silencing; oligonucleotide therapeutic; tumor targeting
Received 29 January 2013; accepted 3 April 2013; advance online publication 14 May 2013. doi:10.1038/mtna.2013.24

The antiapoptotic human B-cell lymphoma 2 (*BCL2*) gene has been a frequent target in studies using ASO and RNA interference technologies[19–24] and plays a role in many cancers, including melanoma[25–29] that has extraordinary intrinsic resistance to apoptotic cell death commonly induced by anticancer drugs, in part due to elevated levels of BCL2.[28,29] We chose a human melanoma xenograft mouse system for its proven track record in predicting efficacy in clinical trials as evidenced by riluzole that has gone on to show efficacy in phase 0 and 2 human trials.[30] Our second target, the metabotropic glutamate receptor 1 (*GRM1*) gene has only recently been established as an important factor in melanoma as well as other cancers.[31–33] Using our novel tumor-specific dendrimer delivery vehicle, we demonstrate that very low doses of anti-*BCL2* or anti-*GRM1* U1 Adaptors are sufficient to reduce growth/progression of human melanoma xenografts with little apparent toxicity. These results offer proof-of-concept that U1 Adaptors are an effective gene-silencing therapeutic platform that can suppress tumor growth using doses far lower than expected based on published experience using other oligonucleotide-based methods.[34] These results also lay a foundation for exploiting U1 Adaptors to target other genes as well as a wide variety of other human disorders.

Results

U1 Adaptor silencing of *BCL2 in vitro*

Twelve anti-human-*BCL2* U1 Adaptors were screened for functional potency in C8161 melanoma cells (**Supplementary Figure S1a,b**). Two U1 Adaptors, BCL2-A and BCL2-B showed strong activity in reducing *BCL2* mRNA levels (**Supplementary Figure S1b,c**) and were used in subsequent studies. LNA- and 2′OMe-modified variants of BCL2-A were compared for activity in C8161 cells (**Figure 1a**, **Supplementary Figure S2a**) and the LNA-modified variant BCL2-A_{L2} showed the highest silencing activity at both the protein (western immunoblots) and mRNA (reverse transcription-quantitative PCR) levels (**Figure 1b** lanes 5–6, **Supplementary Figure S2b**). To demonstrate that the silencing activity of BCL2-A_{L2} is mediated *via* a U1 Adaptor mechanism, C8161 cells were transfected with matching control U1 Adaptors having either the inactivated TD or U1D by mutation or by unlinking the TD and U1D into two separate molecules called "half-Adaptors" (**Figure 1a**). In all cases, these negative controls failed to reduce BCL2 protein (**Figure 1b**) or mRNA (**Supplementary Figure S2b**) levels, strongly supporting a U1 Adaptor-based silencing mechanism, e.g., one where the U1 Adaptor oligonucleotide must tether the target pre-mRNA to the U1 snRNP. Modification of BCL2-A with three PS linkages at each end to improve exonuclease resistance (BCL2-A_{ps}) or a fluorescent label (Cy3-BCL2-A) did not alter potency compared with the parent compound (**Supplementary Figure S2c**).

Development of a tumor-targeting dendrimer nanoparticle

The cyclic RGD pentapeptide (RGD) was chosen as a tumor-targeting ligand because it is small, easy to conjugate, and specifically binds the $\alpha5\beta3$ splice variant of an integrin cell surface receptor that is overexpressed in a wide variety of cancer cells, including C8161.[35,36] The particle was based on a generation 5 (G5) polypropyleneimine (PPI) dendrimer that was previously used to successfully deliver nucleic acid cargos in mouse xenograft models of human tumors.[37–41] As RGD binds to its receptor with much higher affinity as a dimer,[42,43] the RGD targeting ligand was coupled to the PPI G5 dendrimer in a final 2:1 molar ratio to give RGD-G5 (**Figure 1c**). Transfection of C8161 cells *in vitro* with a BCL2-A:RGD-G5 complex demonstrated that RGD-G5 was active as a delivery vehicle, having potency comparable to transfection of BCL2-A with the cationic lipid reagent Lipofectamine 2000 (LF2000) (**Figure 1d**, **Supplementary Figure S3a–c**). Surprisingly, an anti-*BCL2* Dicer-substrate siRNA that was effective using LF2000 transfection did not suppress *BCL2* mRNA levels when used with the RGD-G5 dendrimer, suggesting this delivery vehicle is not compatible with siRNA class reagents (**Figure 1d**). Use of RGD to PPI G5 coupling ratios of 4:1 and 8:1 resulted in reduced efficacy *in vitro* (**Supplementary Figure S4**).

BCL2-A is active *in vivo* and uses a U1 Adaptor mechanism

Mice bearing established C8161 subcutaneous xenografts were administered BCL2-A:RGD-G5 or control complexes in phosphate-buffered saline (PBS) *via* intravenous (iv) tail vein injection. Pilot studies (data not shown) established that effective tumor suppression could be achieved using 1.7 µg of the U1 Adaptor and a 1:1.3 Adaptor:RGD-G5 stoichiometry. Dynamic light scattering measurements indicated the particle size of the injected complex (~3.2 µmol/l U1 Adaptor and ~4 µmol/l RGD-G5 in 1x PBS) was 193 nm with a polydispersion index = 0.18 with little difference in size for different U1 Adaptor sequences (**Supplementary Figure S5**). Mice were given biweekly injections of various formulations for 3 weeks and the tumors were evaluated (**Figure 2a**). Tumor-bearing treatment group 2 (TG2) mice that were dosed with a 1.7 µg BCL2-A:2.4 µg RGD-G5 complex (68 µg Adaptor/kg) per injection exhibited ~70% tumor reduction compared with TG1, the vehicle control group (P = 0.004). No significant tumor suppression was seen with the two control U1 Adaptor cohorts, which were treated with either a TD-mutant BCL2-A (TG3) or a U1D-mutant BCL2-A (TG4). Thus disruption of either the TD or the U1D resulted in loss of activity, strongly arguing for a U1 Adaptor mechanism of action. The TG6 mice were dosed with a 1.7 µg BCL2-A:2.4 µg G5 complex, where G5 matches the RGD-G5 vehicle but lacks the RGD ligand. This cohort did not show reduction in tumor mass, demonstrating the importance of the targeting ligand. Use of a fivefold lower dose (0.34 µg BCL2-A:0.48 µg RGD-G5 complex) resulted in no inhibition of tumor growth (TG5), establishing that >0.34 µg Adaptor/dose was needed for tumor suppression.

Protein and RNA extracted from tumors of day 22 TG1-4 mice demonstrated that only the BCL2-A:RGD-G5–treated mice had reduced BCL2 protein (**Figure 2b**) and mRNA (**Supplementary Figure S6a**). Others have shown that therapeutic-based BCL2 silencing in xenograft mice by either ASOs or siRNAs increases the rate of apoptosis.[19–21,23] Immunohistochemical analysis shown in **Figure 2c** demonstrated that BCL2-A–treated, but not the control animals, showed an increased number of positive, activated Caspase 3 stained

cells. Furthermore, immunohistochemical analysis using the cell proliferation marker, Ki67, showed that BCL2-A–treated, but not the control animals, had a reduced number of actively proliferating cells (**Figure 2d**). Both visual and histopathological inspection of several organs including liver, kidney, spleen, heart, brain, and lung from the TG1-TG6 mice showed no evidence for tissue damage or toxicity (data not shown). None of the mice exhibited overt signs of toxicity such as lethargy, not eating or drinking, loss of body weight or ulceration of the transplanted tumor.

While the above data support that BCL2-A's tumor suppression activity is likely to be mediated through reducing *BCL2* mRNA levels, it did not rule out a possible contribution of an extracellular mechanism such as impaired tumor vascularization, a possible side effect of RGD targeting.[35,36,42,43] This was addressed by showing that C8161 cells transfected with BCL2-A:RGD-G5 *ex vivo* before implantation led to significant tumor suppression (**Figure 2e**). The results of this *ex vivo* experiment strongly suggest that tumor suppression detected *in vivo* is primarily if not completely mediated through an intracellular mechanism and also demonstrate a long-lasting effect as the single *ex vivo* transfection of BCL2-A led to tumor suppression persisting at least through 23 days *in vivo*. C8161 cells transfected with RGD-G5:Adaptor complexes all had a similar doubling time and apoptosis rate (data not shown) independent of whether the Adaptor was

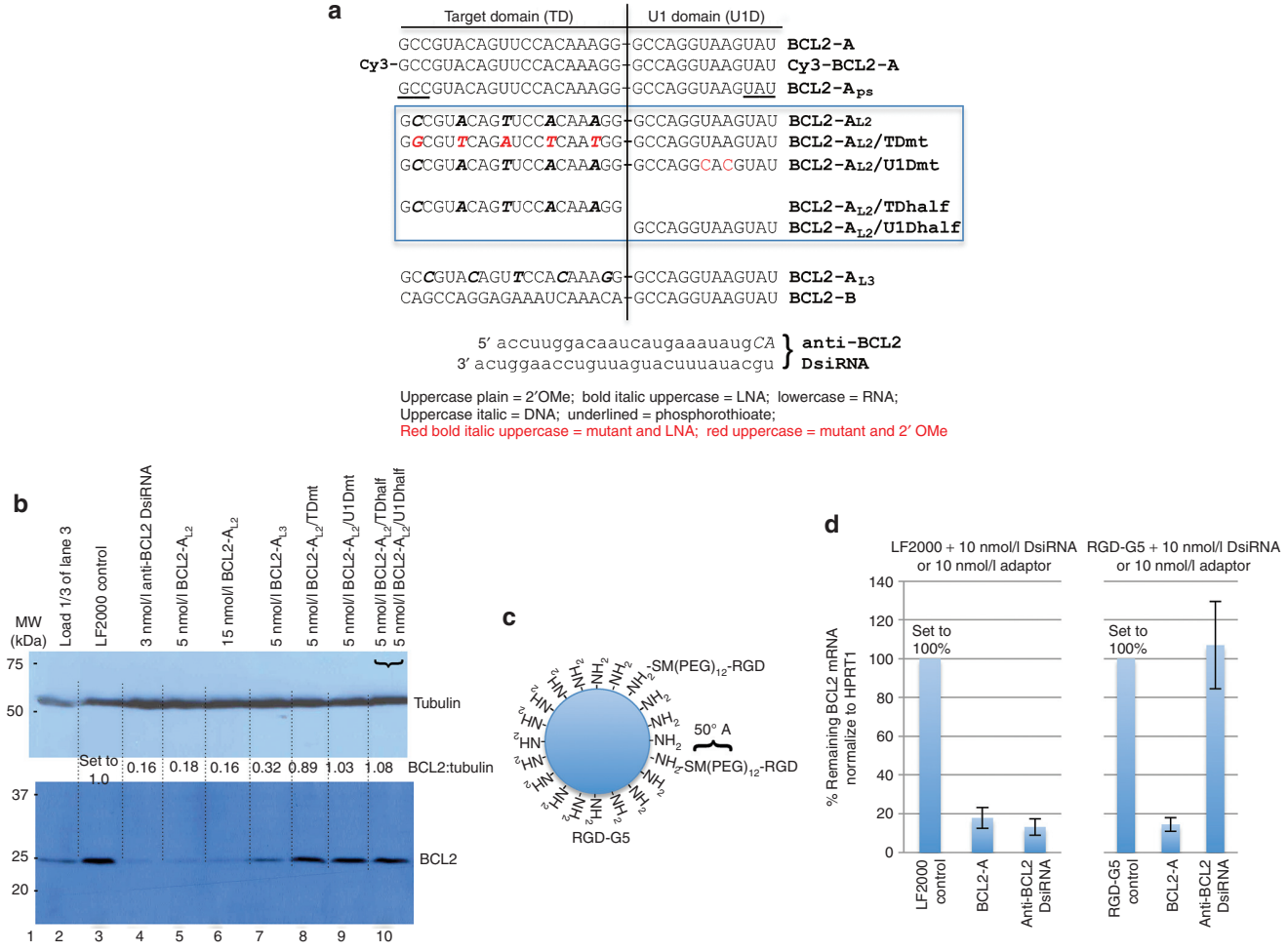

Figure 1 ***In vitro*** **silencing activity of anti-*BCL2* U1 Adaptors and a tumor-targeting nanoparticle**. (**a**) Design and sequences of the BCL2-A and BCL2-B Adaptors, backbone-modified variants of BCL2-A and matching controls as well as an anti-*BCL2* DsiRNA used as a positive control. The boxed region is to indicate a full set of matching control Adaptors. (**b**) The BCL2-A$_{L2}$ U1 Adaptor reduces BCL2 protein. At 24 hours post-transfection of the indicated Lipofectamine 2000 (LF2000):Adaptor or LF2000:anti-*BCL2* DsiRNA complexes, total C8161 lysates were prepared followed by western blot. Lanes 3–10 contain 50 µg/well while lane 2 has 17 µg of protein to show the dose response of the western blot signal. Tubulin was used to show equal loading (top panel) and the lower panel was probed for BCL2. Quantitation of the western signals is shown as a BCL2:tubulin ratio with lane 3 set to 1.0. (**c**) Schematic of RGD-G5 (MW ~9,600) that has a 2:1 RGD to PPIG5 conjugation ratio. For simplicity, only some of the 64 free amino groups of PPIG5 are shown. The attachment positions of the SM(PEG)$_{12}$-linker-RGD group are random and are shown here for illustrative purposes. (**d**) The RGD-G5 nanoparticle (right panel) is comparable to LF2000 (left panel) at delivering the BCL2-A Adaptor to C8161 cells as measured by RT-qPCR of *BCL2* mRNA normalized to *HPRT1*. Note Cq values between the LF2000 control and RGD-G5 control were comparable. DsiRNA, Dicer-substrate small interfering RNA; LNA, locked nucleic acid; MW, molecular weight; RT-qPCR, reverse transcription-quantitative PCR.

capable of silencing BCL2 indicating *in vitro* results do not always predict *in vivo* activities.

Two chemically modified variants of BCL2-A were studied (BCL2-A_{ps} with terminal PS modification and BCL2-A_{L2} with LNA residues in the TD) in an attempt to increase potency *in vivo* (**Figure 3a**). Although BCL2-A_{ps} (TG9) gave significant tumor suppression as compared with the vehicle control (TG7), it was less active than BCL2-A (TG8). BCL2-A_{L2} (TG13) showed tumor suppression equal to BCL2-A, an observation that contrasts with its superior activity *in vitro*,

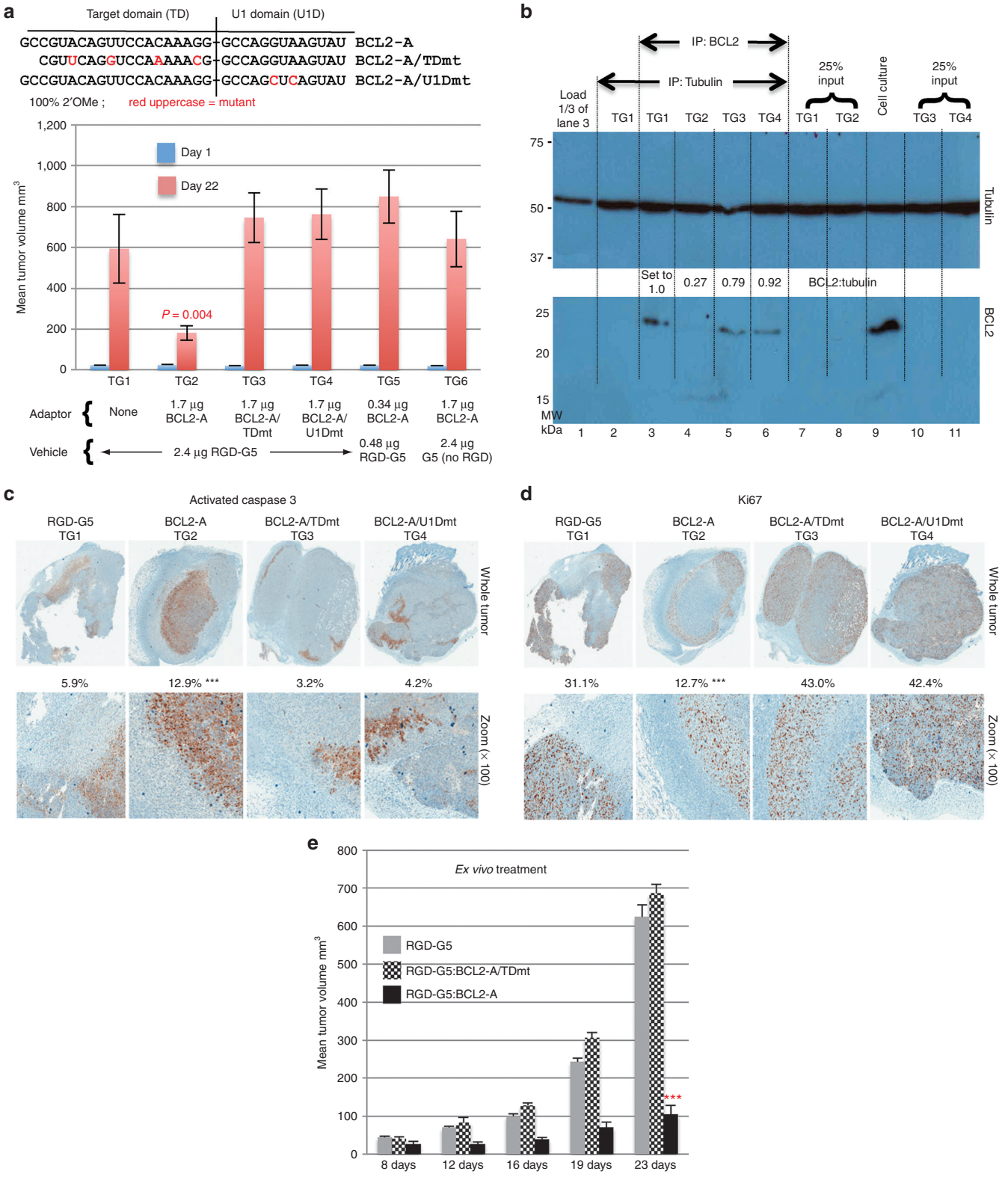

further demonstrating that *in vitro* results do not always translate to similar outcomes *in vivo*. Others have also found unpredictable behavior of LNA backbone modifications.[16,17] The other data in **Figure 3a,b** demonstrated that a 2:1 RGD:PPIG5 coupling ratio was superior to a 4:1 ratio (compare TG8 with TG10); further, a 1:4 Adaptor:RGD-G5 stoichiometry was less effective than a 1:1.3 stoichiometry (compare TG16 with TG18); a minimally effective dose for BCL2-A was 0.85 µg/injection (34 µg Adaptor/kg).

To further support that *BCL2* is indeed the therapeutic target and that the observed tumor suppression was not due to sequence-specific OTEs, we analyzed a second anti-*BCL2* Adaptor (BCL2-B) which targets a different site of the *BCL2* gene. BCL2-B also was effective in reducing tumor mass, albeit with lower potency than BCL2-A (**Figure. 3c**), and used a U1 Adaptor mechanism as single domain mutant BCL2-B Adaptors were not active *in vivo* (**Figure 3d**). Notably, **Figure 3d** used an $(RGD)_{x2}$-containing G5 PAMAM dendrimer (RGD-PAMAM-G5) in place of the PPI core found in RGD-G5 as we wanted to demonstrate that our results were not dependent on a particular class of dendrimer. Indeed a head-head comparison of RGD-G5 and RGD-PAMAM-G5 found they had comparable tumor suppression activity *in vivo* (**Supplementary Figure S6b**). Dynamic light scattering measurements indicated the particle size of the injected complex (~3.2 µmol/l U1 Adaptor and ~4 µmol/l RGD-PAMAM-G5 in 1x PBS) was 200 nm with a polydispersion index = 0.147 with little difference in size for different U1 Adaptor sequences (**Supplementary Figure S4c**). We also demonstrated that BCL2-A's tumor suppression activity is not peculiar to C8161 xenografts as BCL2-A also suppressed UACC903 xenograft tumor growth (**Supplementary Figure S6c**). As compared with C8161, UACC903 is a more aggressive and genotypically distinct melanoma that harbors a V600E *B-RAF* mutation found in 70% of all melanomas (C8161 has a wild-type *B-RAF*).[44,45]

Anti-*GRM1* Adaptors also suppress melanoma tumor growth at low dose

Ectopic expression of *GRM1* in melanocytes is sufficient to induce melanocytic cell transformation *in vitro* and spontaneous melanoma development *in vivo*; short hairpin RNA-based silencing of *GRM1* inhibited tumor cell growth *in vitro* and *in vivo*.[31,46] Screening anti-human–*GRM1* Adaptors in C8161 cells *in vitro* identified three candidate U1 Adaptors that reduced human GRM1 at the protein (**Figure 4a,b**) and mRNA (**Supplementary Figure S7a–d**) levels. Treatment of C8161 xenograft mice with these anti-*GRM1* U1 Adaptors decreased tumor growth and reduced *GRM1* protein levels in day 21 excised xenograft tumors compared with the vehicle control (**Figure 4c**). To demonstrate mechanism of action, the two most potent anti-*GRM1* Adaptors (GRM1-A_{ps} and GRM1-B_{ps}) underwent additional analysis as follows, GRM1-B_{ps} uses a U1 Adaptor mechanism as repeating the GRM1-B_{ps} treatment with matching TD-mutant or U1D-mutant control U1 Adaptors gave no tumor suppression (**Figure 4d**) and no reduction of *GRM1* at the protein and mRNA levels as compared with RGD-G5–treated (vehicle only) control mice (**Figure 4e**). TD and U1D mutant Adaptor control xenograft experiments for GRM1-A_{ps} also demonstrated that the reduced tumor volumes were again mediated by a U1 Adaptor mechanism (**Figure 5a**). Tumor suppression was lost when RGD was replaced with RAD, a well-validated inactive sequence variant of RGD that fails to bind integrin receptors, once again demonstrating that tumor targeting is required. Finally, testing the variant RGD-G5/SPDP vehicle that has a short 10 Å non-PEG–containing linker (in contrast to the 50 Å PEG-linker employed in the original RGD-G5 dendrimer) showed significant reduction in tumor volume, demonstrating that RGD-G5's linker length and composition were not critical for activity.

It was previously shown that short hairpin RNA-based silencing of *GRM1* in human melanoma cell xenografts leads to reduced levels of phosphorylated AKT (pAKT).[46,47] Excised GRM1-A_{ps} U1 Adaptor-treated day 17 tumor samples also showed decreased levels of pAKT (**Supplementary Figure S8**). Immunohistochemical analysis of the excised day 17 tumors from the anti-*GRM1* U1 Adaptor-treated xenografts demonstrated increased activated Caspase 3 and decreased Ki67 staining (**Figure 5b,c**), similar to the previous observation using anti-*BCL2* U1 Adaptors. Both GRM1-A_{ps} and GRM1-B_{ps} U1 Adaptors were also able to suppress tumor progression of UACC903 xenografts, broadening their scope of action to melanoma with mutated B-RAF (**Supplementary**

Figure 2 BCL2-A suppresses tumor growth *in vivo*. (**a**) The design and sequences of the BCL2-A and matching control U1 Adaptors are shown at the top. C8161 xenograft mice were treated when tumor volumes reached ~10 mm^3, which is denoted as day 1. Each treatment group (TG) mouse was treated two times/week consisting of a tail vein injection of 50 µl 1x PBS containing BCL2-A or matching control U1 Adaptors in complex with the RGD-G5 vehicle or the G5 vehicle that lacked RGD (TG6). The only TG that showed significant tumor suppressive activity was TG2 in comparison with TG1. Note that 1.7 µg Adaptor is ~0.16 nmol, 2.4 µg RGD-G5 is 0.2 nmol. (**b**) Immunoprecipitation (IP)-western blot of day 22 excised tumor samples. Due to the low BCL2 signal in standard western blots using excised tumor lysates in comparison to cultured cells (compare lane 9 with lanes 7–8, 10-11), we performed anti-BCL2 IP in lanes 3–6 before the western blot. Antitubulin IP was also done in lanes 3–6 to internally control for IP efficiency. Lane 2 was antitubulin IP only to show the specificity of the BCL2 IP signals. Lane 1 had 3x less protein than lane 3 to show the dose response of the IP-western blot signals. Levels of BCL2 protein were comparable in TG1, TG3, and TG4 (lanes 3, 5, and 6) whereas TG2 (lane 4) BCL2 levels were barely detectable. Quantitation of the western signals is shown in lanes 3–6 as a BCL2:tubulin ratio with lane 3 set to 1.0. (**c**,**d**) Immunohistochemistry of day 22 excised tumor samples for TG1-4 mice with (**c**) activated Caspase 3 as a measure of cellular apoptosis and (**d**) Ki67 as a measure of proliferation. The entire slide ("Whole Tumor" image, ×10 original magnification) was counted and the percent of positive cells is given below the image. The *P* value was only significant for TG2 as compared with TG1. The "Zoom" images are a representative ×100 original magnification image of the whole tumor. In **c** and **d**, ***$P < 0.0001$ when compared with the TG1 vehicle control. (**e**) Tumor volumes of *ex vivo*-treated C8161 xenograft mice. One day before tumor cell implantation, C8161 were transfected as per **Figure 1d** with the following complexes: RGD-G5 as the vehicle control, BCL2-A/TDmt:RGD-G5 as an inactive Adaptor control, or BCL2-A:RGD-G5. After 24 hours, cells were prepared and 1 million cells were subcutaneously implanted into each flank of each mouse. Tumor growth was then monitored for 23 days when the experiment was terminated. ***$P < 0.0001$ when the tumor volumes of BCL2-A:RGD-G5 were compared with the RGD-G5 vehicle controls. MW, molecular weight.

Figure S9a). In contrast to previous observations using BCL2-A, the presence of PS end-modifications on the anti-*GRM1* U1 Adaptors resulted in superior *in vivo* activity compared with the same oligonucleotides with phosphodiester end linkages (**Supplementary Figure S9b**).

No toxicity or immune stimulation was observed in U1 Adaptor-treated C57BL6 mice

It was important to examine the effects of U1 Adaptor administration in immune-competent mice (C57BL6) to directly assess whether the U1 Adaptor antitumor effects could in part be based on stimulation of the innate immune system, a complication observed using other gene-silencing therapeutics.[48–50] Although a variety of receptors will recognize various forms of DNA and RNA, no receptors are known that recognize 2′OMe RNA or LNA residues, making it unlikely that the U1 Adaptors employed in the present study would trigger immune activation. BCL2-A and GRM1-A_{ps} U1 Adaptor:RGD-G5 complexes were injected into C57BL6 mice; interleukin-12 (IL-12) and interferon-α (IFN-α) levels were measured

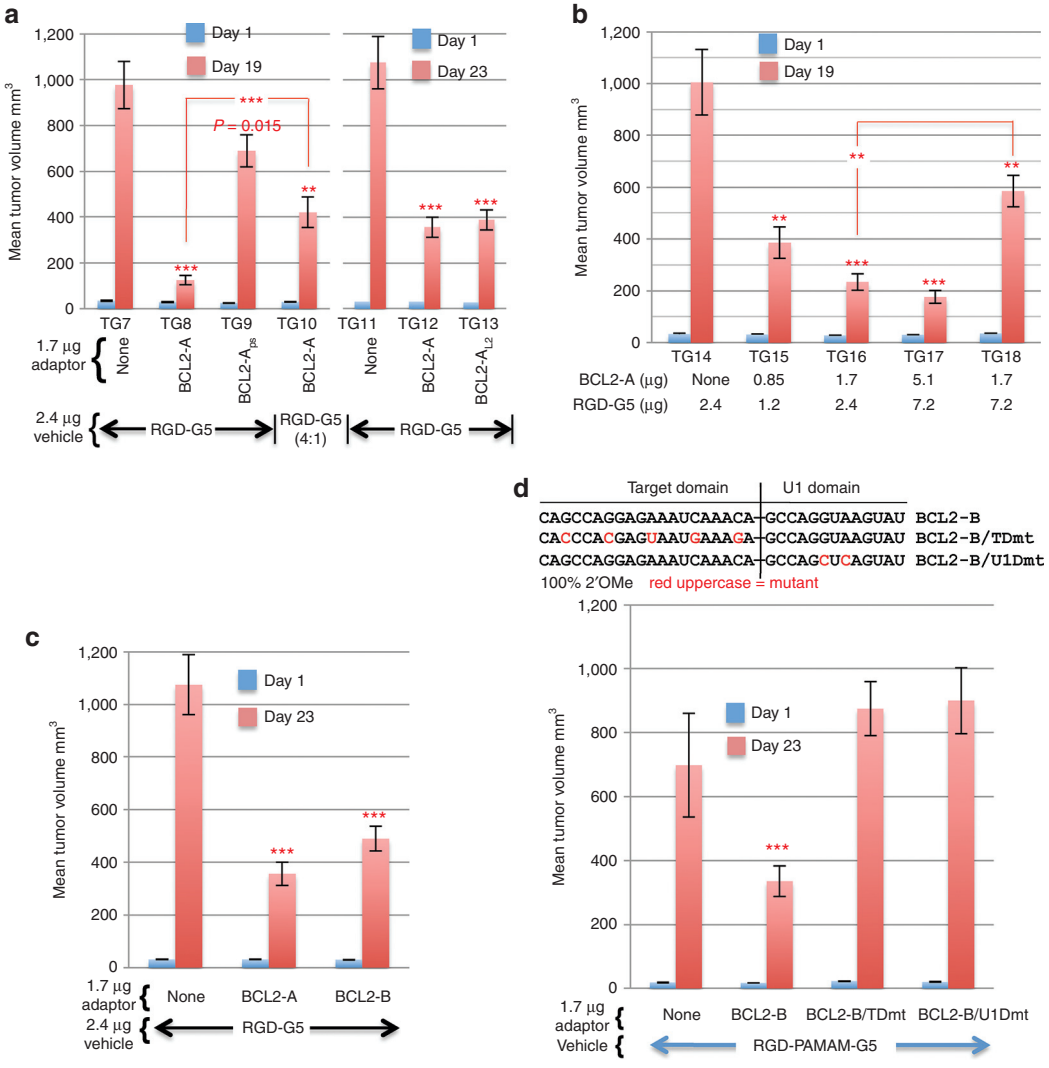

Figure 3 Tumor suppression activity of various anti-*BCL2* U1 Adaptors. (**a**) Tumor volumes of C8161 xenografts are shown with the Adaptor sequences given in **Figure 1a**. Except for the indicated differences, these tumor suppression experiments and statistics are as described in **Figure 2a**. The left and right panels are from experiments done at different times. Treatments of TG10 mice matched those of TG8 except the RGD-G5 vehicle had a 4:1 rather than 2:1 RGD:G5 ratio. The bracket is the *P* value of TG10 versus TG8. All other *P* values (***$P < 0.0001$ and **$P < 0.001$) were calculated as compared with either the TG7 vehicle control (left panel) or the TG11 vehicle control (right panel). (**b**) Dose response studies for treatment of C8161 xenografts. Except for the indicated differences, these tumor suppression experiments, statistical analysis, and symbols are as in **Figures 2a** and **3a**. The bracket is the TG18 versus TG16 *P* value that shows a significant reduction in efficacy when using 3x more RGD-G5 vehicle than U1 Adaptor. All other *P* values (***$P < 0.0001$ and **$P < 0.001$) were calculated as compared with the TG14 vehicle control. (**c**) Shows the tumor suppression activity of BCL2-B in C8161 xenografts as compared with BCL2-A. Except for the indicated differences, these experiments are as described in **Figures 2a** and **3a**. (**d**) Shown are the design and sequences of the BCL2-B and matching control U1 Adaptors and their *in vivo* tumor suppression activities in C8161 xenograft mice. Except for the indicated differences and the use of 8 µg (0.2 nmol) RGD-PAMAM-G5 nanoparticle in place of 2.4 µg (0.2 nmol) RGD-G5, these experiments and symbols are as described in **Figures 2a** and **3a** and the *P* values calculated as compared with the vehicle only control. In **c** and **d**, ***$P < 0.0001$ and **$P < 0.001$ when compared with the corresponding vehicle control.

4 hours post-injection. Baseline levels of both cytokines were seen for all mice except those in the positive control cohort which were administered poly(I:C), a known toll-like receptor 3 (TLR3) agonist (**Figure 6a** and **Supplementary Figure S10**).[51] In a similarly designed but independent experiment, baseline levels of IL-12 and interferon-α were also observed 24 hours post-injection (**Supplementary Figure S11a,b**). C57BL6 mice were given the standard 3-week U1 Adaptor treatment regimen (68 µg Adaptor/kg; two times/week) and serum levels of alkaline phosphatase and alanine transaminase were measured to assess for evidence of hepatic injury; both enzymes remained at basal levels throughout the study period (**Figure 6b,c**). These same serum samples also contained basal levels of IL-12 and IFN-α levels indicative of no immune stimulation even after 3 weeks of biweekly treatments (data not shown). Six organs from the same mice (liver, kidneys, spleen, heart, brain, and lungs) were excised, stained, and analyzed by the Rutgers-UMDNJ Molecular Histopathological Facility Core. No tissue damage was detected and only rare foci of inflammatory cells were seen in all organ samples. Thus no evidence for toxicity was found for any treatment group.

Discussion

U1 Adaptors were previously shown to be effective triggers of gene silencing in mammalian cells *in vitro* but their applicability for *in vivo* use was heretofore untested. The present study offers proof-of-concept that U1 Adaptors can be effective in suppressing expression of targeted genes and slow tumor growth *in vivo* when combined with a suitable delivery vehicle. Success was observed using the same xenograft mouse system and human cell lines (C8161 and UACC903) that proved predictive for riluzole in preclinical studies that later went on to show efficacy in phase 0 and 2 human trials.[30] The broad utility of the U1 Adaptor approach is underscored by the fact we successfully targeted two genotypically different melanoma cell lines (BRAF wild-type and BRAF V600E mutant) and two different cancer-implicated genes, *BCL2* and *GRM1*. The technology also proved robust as our very first *in vivo* experiment and all subsequent experiments, encompassing ~108 treatment groups totaling over 800 mice, exhibited a very high potency for both genes, suppressing tumor progression at doses as low as 34–68 µg Adaptor/kg. U1 Adaptors have two distinct functional domains, both of which must be present on the same oligonucleotide to function *via* a U1 snRNP-based mechanism of action. Suitable negative controls for mechanism of action include use of full-length U1 Adaptors with mutations in either the TD or the U1D or half-Adaptors (isolated TD or U1D) to show that both functional domains must reside on the same molecule.[7] The present study employed all of these mechanistic controls and demonstrated that an intact U1 Adaptor oligonucleotide with functional (*i.e.,* non-mutated) sequences in both the TD and U1D is required to achieve tumor suppression and a gene suppression effect. These controls further support a U1 mechanism of action in both the *in vitro* and *in vivo* studies.

Tumor growth can be suppressed by a variety of routes including downregulation of necessary oncogenes, nutritional starvation (disruption of vascular supply), direct chemical cytotoxicity, or immune activation. In the present study, we found evidence for induction of apoptosis and reduced cell division only in tumor-bearing animals treated with intact (non-mutated) anti-*BCL2* or anti-*GRM1* U1 Adaptors, which correlated with reduction of BCL2 or GRM1 levels in the tumor tissue. Treated animals showed no evidence for either general chemical toxicity from the administered compounds or immune activation. Further, tumor cells treated *ex vivo* with the U1 Adaptors before implantation showed marked growth retardation in animals that never received iv dosing of the U1 Adaptor:RGD-G5 complex, making it unlikely that disrupted vascularization contributed to tumor suppression.

U1 Adaptors are large, highly charged synthetic nucleic acids with a molecular weight of around 11,000 daltons. Molecules of this type do not readily enter most cell types without assistance, so use of an appropriate delivery vehicle is crucial to the success. The need for efficient delivery, one of the primary challenges of the oligonucleotide therapeutic field, continues to inspire production of an ever-widening variety of delivery systems ranging from cationic lipid or polymer-based nanoplexes, to antibody-protein fusion systems, to encapsulation of the oligonucleotide drug in exosomes or bacterial minicells. With the exception of delivery to liver,[34,52,53] efficacious siRNA-based targeting using low microgram doses is usually not possible with systemic iv dosing and typically is only seen with local administration (e.g., direct intraocular or intratumoral injection). Use of dendrimers to deliver therapeutic oligonucleotides is relatively under-explored, although a recent report successfully used a PAMAM dendrimer to deliver therapeutic doses of multiple Dicer-substrate siRNAs at single digit microgram levels in a humanized mouse model of HIV1.[54] Although the PPI dendrimer-based system employed here was useful in this proof-of-concept study and exhibited no detectable toxicity, it is clearly prudent to explore the compatibility of other delivery systems with U1 Adaptors. It is important to acknowledge the contribution of ligand targeting for the success we observed using the present dendrimer-based systems. The low-dose efficacy achieved here required the RGD targeting ligand and tumor suppression was lost when the RGD ligand was either omitted from the vehicle or substituted with the related but inactive RAD variant.

To date, most reports targeting *BCL2* with siRNAs and ASOs in tumor-bearing mice have involved injection of a naked oligonucleotide, precluding comparison with the work presented here. Systemic injection in tumor-bearing mice of 10 mg doses of a naked anti-*BCL2* ASO was efficacious leading to phase 3 trials that ultimately failed due to poor efficacy.[2,27] Systemic injection of a naked anti-*BCL2* siRNA at 200 µg/kg daily for 24 days led to tumor suppression in human Panc1 (pancreatic) mouse xenografts.[22,23] Of particular interest was a dual functional siRNA that suppressed *BCL2 via* an RNA interference mechanism while activating RIG-1 expression and an immune response through a 5′ end triphosphate group with a combined efficacy at 50 µg doses delivered on days 3, 6, and 9 in a mouse melanoma model in C57BL6 mice.[55] However, the complex chemistry needed to produce triphosphate siRNAs may preclude the scale-up needed for clinical studies. While the RGD ligand used here was chosen for its simplicity and prior success when used at

very low doses to image human tumors growing in mice,[56] there are many other tumor-targeting ligands that may prove superior. Although concern has been raised about the non-specific effects of RGD when used at high doses,[43] this may be largely alleviated at far lower doses such as the ones reported here.

The achievement of proof-of-concept paves the way for future studies including exploration of pharmacodynamic and pharmacokinetic properties as well as expanded dose response studies and the use of other delivery systems/targeting ligands. Previous *in vitro* work found that, unlike siRNAs where the most potent siRNA in a pool appears to dominate the functional response,[57,58] the combined use of several U1 Adaptors against the same target increased the level of gene suppression.[7] The use of multiple U1 Adaptors against the same target may permit even lower dosing to be used, which could be beneficial if dose-related toxicity or other OTEs were found in a different system. Further,

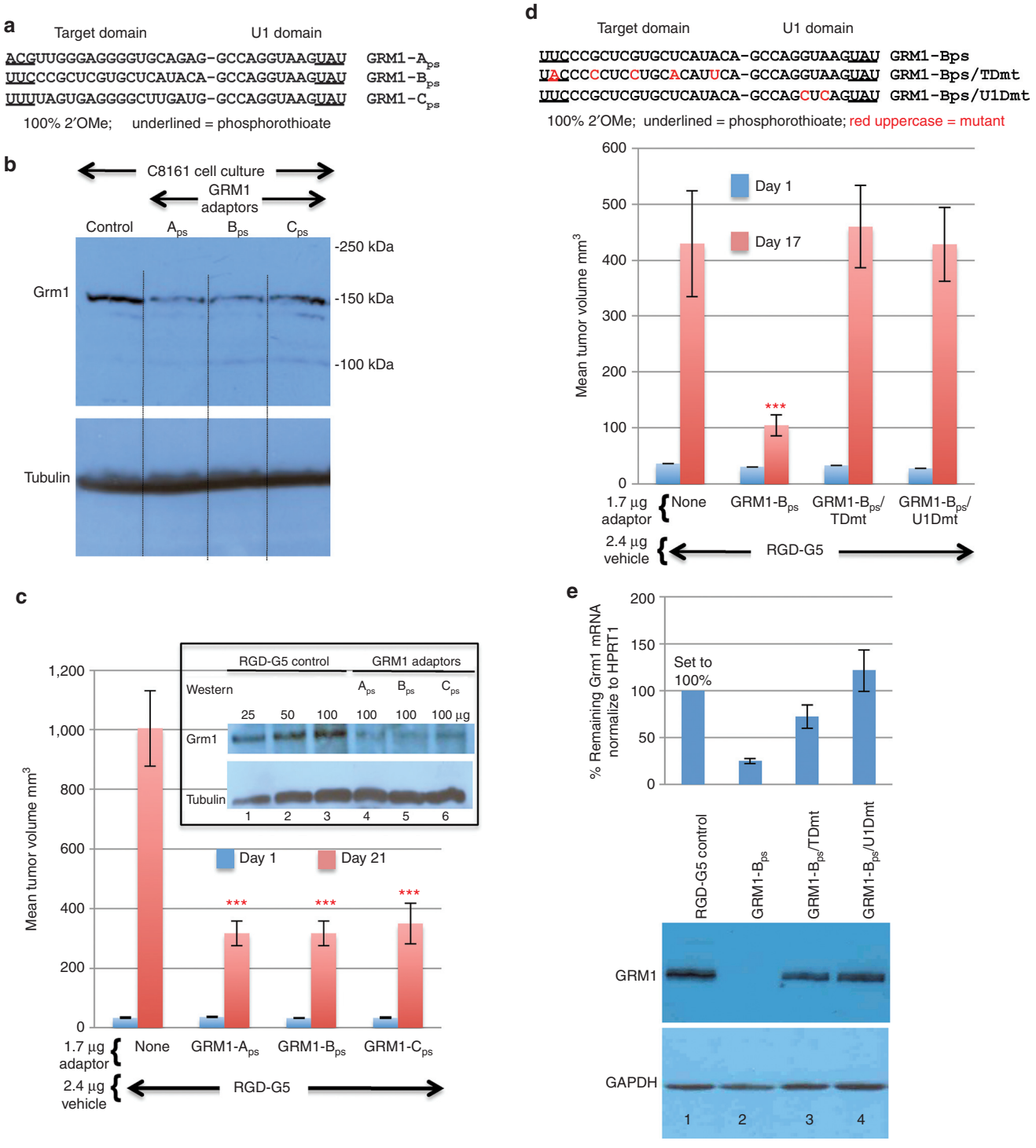

Figure 4 Anti-*GRM1* U1 Adaptors are active *in vitro* and suppresses tumor growth *in vivo*. (**a**) The design and sequences of three anti-*GRM1* U1 Adaptors made of 2′OMe RNA with three phosphorothioate internucleotide linkages at each end. (**b**) Western blot demonstrating the anti-*GRM1* U1 Adaptors reduce GRM1 protein levels in cultured C8161 cells. Transfection and western blotting are as in **Figure 1b** except C8161 lysates were prepared at 72 hours post-transfection and 50 µg/lane were separated by 8% SDS-PAGE. The transfection and western blots were repeated three times with similar results. (**c**) Shown are the *in vivo* tumor suppression activities of the anti-*GRM1* U1 Adaptors in C8161 xenograft mice. Except for the indicated differences, these experiments are as described in **Figures 2a** and **3a** and the *P* values calculated as compared with the vehicle only control. The insert is a western blot of excised day 21 tumor samples with amounts of total tumor protein loaded per lane indicated (note, unlike **Figure 2b** for *BCL2* where IP-western blot performed, this is a regular western blot). Lanes 1 and 2 contained less protein to show the dose response of the western blot signals. Tubulin was used to show equal loading. (**d**) The design and sequences of the GRM1-B_{ps} and matching control U1 Adaptors and their *in vivo* tumor suppression activities in C8161 xenograft mice. Except for the indicated differences, these experiments are as described in **Figures 2a** and **3a** and the *P* value calculated as compared with the vehicle only control. In **c** and **d**, ***$P < 0.0001$ when compared with the corresponding vehicle control. (**e**) To assess *GRM1* expression, protein and RNA were extracted from excised (as shown in **d**) day 17 tumors and analyzed by RT-qPCR (upper panel) or western blot (lower panel). The experiments were done three times with similar results. GAPDH, glyceraldehyde 3-phosphate dehydrogenase; RT-qPCR, reverse transcription-quantitative PCR; TD, target domain; U1D, U1 domain.

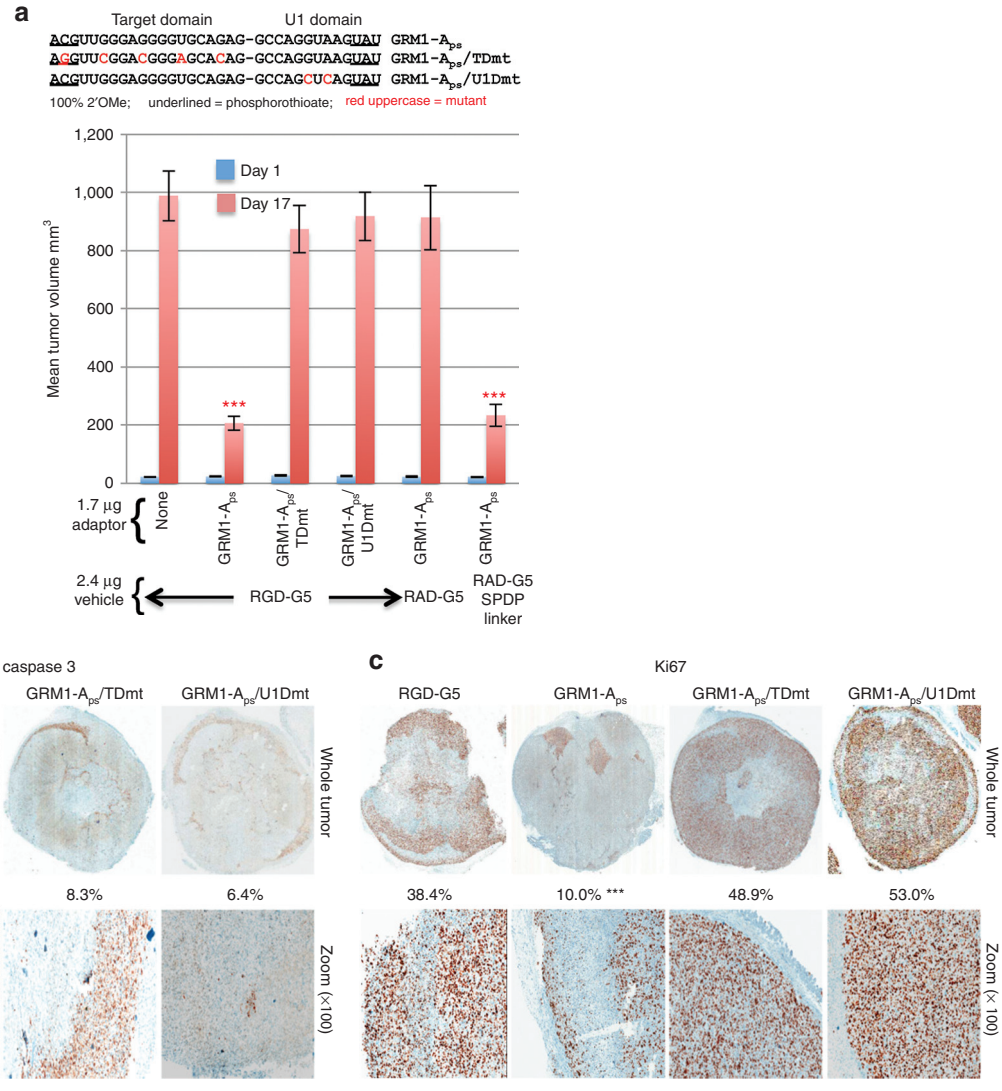

Figure 5 Mechanism of anti-*GRM1* U1 Adaptors. (**a**) Shown are the design and sequences of the GRM1-A_{ps} and matching control U1 Adaptors and their *in vivo* tumor suppression activities in C8161 xenograft mice. Except for the indicated differences, these experiments and symbols are as described in **Figures 2a** and **3a** and the *P* values calculated as compared with the vehicle only control. Treatments for the GRM1-A_{ps}:RAD-G5 group matches that of the GRM1-A_{ps}:RGD-G5 group except the RGD peptide was replaced with an RAD peptide that has lost binding to the receptor. Treatments for the GRM1-A_{ps}:RAD-G5-SPDP linker group matches that of the GRM1-A_{ps}:RGD-G5 group except the former nanoparticle had a far shorter linker and non-PEGylated chemistry as described in the text and Materials and Methods section. (**b**,**c**) IHC of excised day 17 tumor samples from **Figure 5a** mice to assess levels of (**b**) activated Caspase 3 as a measure of apoptosis and (**c**) Ki67 as a measure of proliferation. Symbols and quantitation are as described in **Figure 2c,d**. In **a**–**c**, ***P < 0.0001 when compared with the corresponding vehicle control. IHC, immunohistochemistry; TD, target domain; U1D, U1 domain.

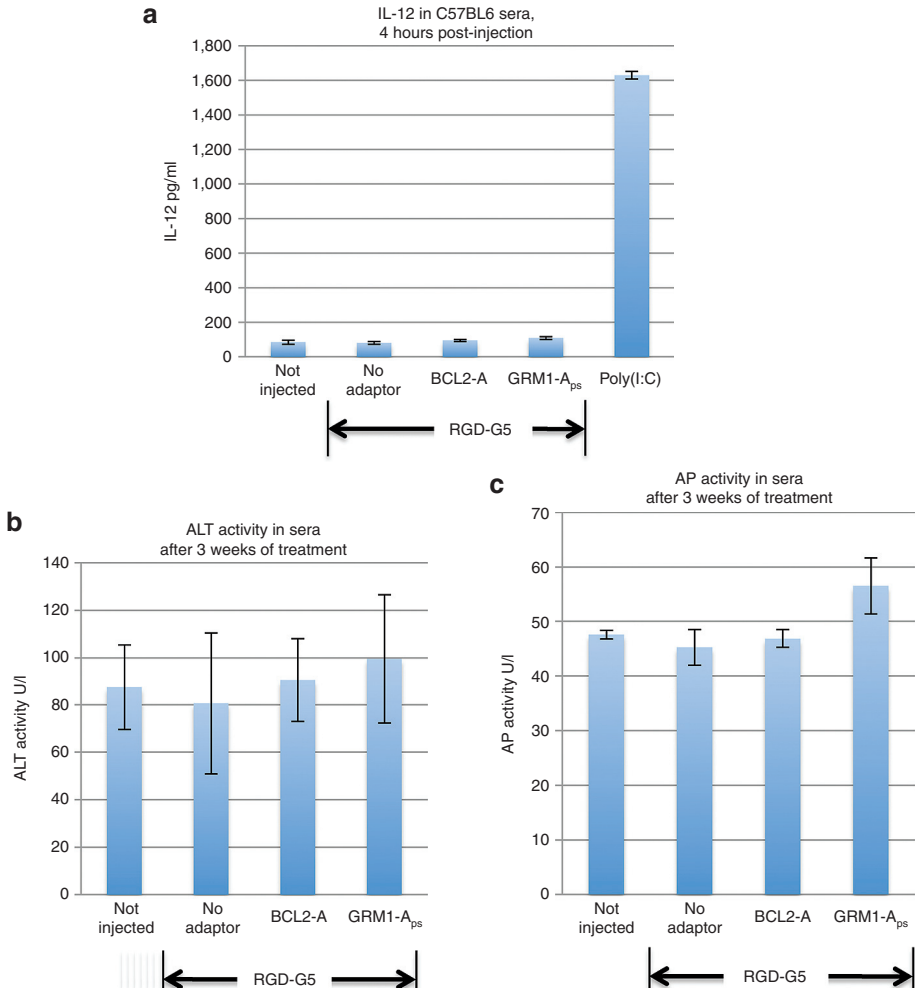

Figure 6 U1 Adaptor treatment does not elicit immune responses or increase liver enzyme activity in C57BL6 mice. (**a**) C57BL6 male mice (five mice/group) underwent a single tail vein injection with the standard dose of 1.7 µg Adaptor:2.4 µg RGD-G5 complex or just 2.4 µg RGD-G5 vehicle alone. The first group was not injected. Poly(I:C) was injected as a positive control.[51] At 4 hours post-injection, blood was drawn and IL-12 levels were measured as well as IFN-α levels (**Supplementary Figure S10**). (**b**,**c**) C57BL6 male mice (five mice/group) underwent 3 weeks of standard U1 Adaptor treatment as described in **Figure 2a** with two times/week dosing with a 1.7 µg Adaptor:2.4 µg RGD-G5 complex or just 2.4 µg RGD-G5 vehicle alone. The first group of mice was not injected. At 48 hours after the final injection, blood was drawn and levels of the (**b**) ALT and (**c**) AP liver enzymes were measured. ALT, alanine transaminase; AP, alkaline phosphatase; IFN-α, interferon-α; IL, interleukin.

considering that clinical responses are not durable and relapse is a near-certainty for most cancers using monotherapy, the possibility of simultaneous multi-gene targeting with multiple U1 Adaptors to achieve higher levels of tumor cell apoptosis and longer lasting tumor suppression is an attractive option. Combinational therapy combining U1 Adaptors and small molecule chemotherapeutic agents is also expected to provide enhanced therapeutic benefit, an approach already shown to be successful for siRNAs[23] and ASOs.[21,24,27]

Materials and methods

Xenografts in immunodeficient nude mice. All animal studies were approved by the Institutional Review Board for the Animal Care and Facilities Committee of Rutgers University. Male nude mice (5 weeks old) were purchased from Taconic (Hudson, NY). Human melanoma cells, C8161 or UACC903, were injected into the dorsal area at 10^6 cells per site. Unless indicated, all treatment groups comprised 10 mice. Tumors were measured weekly with a Vernier caliper and tumor volume (V; cubed centimeters) was calculated by using the equation $V = d^2x \cdot D/2$, where d (centimeters) and D (centimeters) are the smallest and largest perpendicular diameters. Once tumors reached ≈10 mm^3, the animals were divided randomly into treatment groups so that the mean difference in tumor size between each group was <10%. Mice were killed after ~3 weeks (for C8161) or ~5 weeks (for UACC903) corresponding to when the tumor volume in the vehicle-treated group had reached the maximum size permitted by the institutional review board. The tumor xenografts were excised for further histological and molecular analyses. *P* values were calculated using Student's two-tailed *t*-test.

Preparation and analysis of RNA, proteins, and source of oligonucleotides. RNA and protein levels from transfected cells and excised tumors from xenografts were determined by western blotting and reverse transcription-quantitative PCR as previously described,[7,31] except for the immunoprecipitation (IP) western blot (described below). The quantitative PCR primers, siRNAs, and gene-specific U1 Adaptors were manufactured by Integrated DNA Technologies (IDT, Coralville, IA) except for the LNA-containing Adaptors, which were purchased from Exiqon (Vedbaek, Denmark). The Control U1 Adaptor used is a 2′OMe-modified oligonucleotide not complementary to human transcripts 5′-GUCAGAAAUACA CAAUACCUGCCAGGUAAGUAU derived from a reporter transcript described in ref. 7. Poly(I:C) (VacciGrade) was purchased from Invivogen (San Diego, CA).

IPs and western blots. IP of protein from excised tumors was done as follows with all steps done at 4 °C. Protein G beads (catalog 17-0618-01; GE Healthcare, Pittsburgh, PA) were prepared by washing 3x in TNET (20 mmol/l Tris pH 7.4, 150 mmol/l NaCl, 1 mmol/l EDTA, 1% triton X-100), followed by 1 hour TNET + 1 mg/ml bovine serum albumin, followed by three washes in TNET and resuspended as a 50% slurry in TNET. Each IP sample contained 500 µg of tumor protein diluted to 300 µl with TNET containing protease cocktail inhibitors II, III, and IV (Calbiochem catalog nos. 524625, 539134, and 524628; Merck KGaA, Darmstadt, Germany) diluted as per the manufacturer's instructions. To each IP sample in **Figure 2b**; lanes 3–6, was added 8 µl anti-BCL2 antibody (Invitrogen catalog 13-8800; Life Technologies, Carlsbad, CA) and 1 µl antitubulin antibody (catalog AB-2/DM1A; Abcam, Cambridge, MA), except for lane 2 that had only antitubulin antibody. After gentle rocking for 4 hours, 20 µl protein G bead slurry (10 µl packed beads) was added and the sample gently rocked for four more hours. The beads were gently pelleted, the supernatant aspirated and the beads washed three times in TNET with a 5-minute rocking/wash. After removing the last of the supernatant, the beads were resuspended in laemmli loading buffer, heated and analyzed by 12% western blot. The upper half of the membrane was probed with antitubulin antibody. To avoid interference with the mouse light chain signal that migrates close to the BCL2 band, the lower half of the membrane was probed with anti-BCL2 from rabbit (SAB4300340; Sigma-Aldrich, St Louis, MO).

Immunohistochemistry. The Tissue Analytical Services at the Cancer Institute of New Jersey performed all the immunohistochemical staining of excised tumor xenografts to detect changes in the number of apoptotic and proliferating cells using the well-known activated Caspase 3 and Ki-67 markers, respectively. The number of stained cells was quantified with a digital Aperio ScanScopeGL system and ImageScope software (v 10.1.3.2028) (Aperio Technologies, Vista, CA) according to the manufacturer's protocol with modifications as described.[59]

Immune response and liver enzyme assays. IL-12 and IFN-α levels in mouse serum samples were measured using specific ELISA kits from Invitrogen (Life Technologies) and PBL Interferon Source (Piscataway, NJ), respectively. The activities of alanine transaminase and alkaline phosphatase in mice serum were determined using the MaxDiscovery ALT enzymatic assay kit and MaxDiscovery AP enzymatic assay kit (Bioo Scientific, Austin, TX) according to the manufacturer's instructions.

Statistics. The number of mice used for each experiment was determined with the help from the Biometrics Facility Core at the Cancer Institute of New Jersey. *P* values were determined using unpaired Student's two-tailed *t*-test. Xenograft experiments comprised 10 mice/group except in a few cases where 5–8 mice/group were used. With 10 mice per group, a 35% treatment difference between control and tested group can be detected with 80% power at an α-level of 5% (two-sided test). A *P* value of <0.05 was considered significant.

Preparation of RGD-G5 nanoparticles. PPIG5 (SyMO-Chem, Eindhoven, Netherlands) was diluted to a 10 mmol/l stock in water using HCl to bring the pH to 7.0 and stored in aliquots at –80 °C. cRGD and cRAD (Peptides International, Louisville, KY), and the $SM(PEG)_{12}$ and LC-SPDP linkers (Thermo Scientific Pierce, Rockford, IL) were resuspended and stored as per the manufacturer's instructions. Conjugation to make RGD-G5 was as follows: 24 µl of 200 mmol/l $SM(PEG)_{12}$ in DMSO was added to 6.1 ml of 0.25 mmol/l PPIG5 in aqueous buffer containing 50 mmol/l KCl, and incubated for 1 hour at room temperature, ($SM(PEG)_{12}$ was threefold excess over PPIG5). Glycine was then added to a final 3 mmol/l concentration to neutralize any unreacted $SM(PEG)_{12}$ and after 30 minutes the solution brought to 40 mmol/l Tris pH 6.8 and a sixfold excess cRGD added to a final 1.5 mmol/l concentration. After 1 hour of conjugation, excess cysteine was added to neutralize any unreacted groups and the sample extensively dialyzed 48 hours with three changes of buffer against 30 mmol/l Hepes pH 7.9. The final sample was 200 µmol/l RGD-G5 in 30 mmol/l Hepes pH 7.9 and was stored in aliquots at –80 °C. Multiple freeze thawing (>20) had no detectable effect on activity.

Preparation of RGD-G5/SPDP, a short, non-PEG–containing linker version of RGD-G5. RGD-G5/SPDP was prepared as follows: 8 ml of 0.25 mmol/l PPIG5 in 10 mmol/l Hepes pH 7.9, 1 mmol/l EDTA, and 1.5 mmol/l LC-SPDP (added last) was incubated for 2 hours at room temperature. After overnight dialysis with two changes of buffer against 10 mmol/l Hepes pH 7.9, 1 mmol/l EDTA, a pyridine 2-thione release assay was done as per the manufacturer's instructions to determine the conjugation efficiency. Then 500 µl of 5 mg/ml cRGD freshly dissolved in 3% acetic acid was added to 7.3 ml of the activated PPIG5 and the reaction proceeded overnight at 4 °C. After overnight dialysis with two changes of buffer against 10 mmol/l Hepes pH 7.9, 1 mmol/l EDTA, a pyridine 2-thione release assay was done and the final samples stored in aliquots at –80 °C.

Dynamic light scattering. Particle size of the injected formulation at standard dose either a 1.7 µg (3.2 µmol/l) U1 Adaptor:2.4 µg (4 µmol/l) RGD-G5 complex in 1x PBS or a 1.7 µg (3.2 µmol/l) U1 Adaptor:8 µg (4 µmol/l) RGD-PAMAM-G5 complex in 1x PBS was determined by a DLS apparatus (Malvern Zetasizer; Malvern Instruments, Westborough, MA). Several dilutions of the sample were analyzed by automatic

measurement setting comprised of the average of runs, each run having 30 measurements of 5 seconds per measurement.

Preparation of RGD-PAMAM-G4 and RGD-PAMAM-G5. PAMAM-G4 and PAMAM-G5 (Dendritech, Midland, MI) were diluted to a 2 mmol/l stock in water using HCl to bring the pH to 7.0 and stored in aliquots at –20 °C. RGD-PAMAM-G4 was prepared as follows: 1 ml of 0.2 mmol/l PAMAM-G4 in 25 mmol/l Hepes pH 7.9, 1 mmol/l EDTA, 150 mmol/l NaCl, and 1.2 mmol/l LC-SPDP (added last) was incubated for 2 hours at room temperature. After overnight dialysis with two changes of buffer against 25 mmol/l Tris pH 8.0, 1 mmol/l EDTA, and 150 mmol/l NaCl, a pyridine 2-thione release assay was done as per the manufacturer's instructions to determine the LC-SPDP conjugation efficiency. Then 23.2 µl of 25 mg/ml cRGD freshly dissolved in 3% acetic acid was added to 1.3 ml of the activated PAMAM-G4 and the reaction allowed to proceed overnight at 4 °C. A pyridine 2-thione release assay was done to measure cRGD coupling efficiency. After overnight dialysis with two changes of buffer against 1x PBS, the final samples were stored in aliquots at –80 °C. The same protocol was used to prepare RGD-PAMAM-G5.

Calculation of the RGD:PPIG5 ratio. The number of RGD's linked to PPIG5 was determined in several ways. First, the colorimetric bicinchoninic acid protein assay (Thermo Scientific Pierce) that measures reduction of Cu^{2+} to Cu^{1+} by the RGD peptide was used. Second, RGD-G5 and RGD-G5/SPDP underwent MALDI-MS analysis using as a matrix 2,4,6-Trihydroxyacetophenone (THAP) in 50% acetonitrile in 50 mg/ml ammonium acetate. Third, the LC-SPDP linker used to make RGD-G5/SPDP permits conjugation efficiency by monitoring pyridine 2-thione release at 343 nm as per the manufacturer's instructions. All of these methods led to close agreement that an average of two RGD's were coupled to each PPIG5.

Cell culture and transfection. C8161 and UACC903 cells were grown in RPMI medium supplemented with 10% fetal bovine serum and antibiotics. Cationic lipid-based transfection with LF2000 was done as previously described.[7] Transfection with RGD-G5 dendrimer was done as follows. For a 6-well plate, a 0.2 ml transfection mix containing 1x PBS pH 7.2 was prepared. RGD-G5 was diluted into 180 µl PBS and then the Dicer-substrate siRNA or U1 Adaptor was added to give a final volume of 0.2 ml in 1x PBS, and the solution gently mixed. After 5 minutes at room temperature, the RGD-G5:oligonucleotide complexes were added to cells that had been overlaid with 1.8 ml of fresh growth media. For larger or smaller scale transfections, the transfection mix was scaled accordingly. After the indicated time, cells were harvested and protein and/or RNA was extracted.

Supplementary material

Figure S1. *In vitro* silencing activity of anti-*BCL2* U1 Adaptors.
Figure S2. *In vitro* silencing activity of variants of the BCL2-A Adaptor.
Figure S3. *In vitro* dose response silencing activity of the BCL2-A Adaptor complexed with the RGD-G5 nanoparticle.
Figure S4. *In vitro* silencing activity of various dendrimer:BCL2-A Adaptor complexes.
Figure S5. Particle size of various dendrimer:BCL2-A Adaptor complexes.
Figure S6. Analysis of BCL2-A activity in C8161 and UACC903 xenografts.
Figure S7. *In vitro* silencing activity of anti-*GRM1* U1 Adaptors and matching controls.
Figure S8. Western blot analysis to assess the level of pAKT versus AKT in day 17 tumors from anti-*GRM1* U1 Adaptor-treated mice.
Figure S9. The anti-*GRM1* Adaptors suppress growth of UACC903 xenografts and terminal PS bonds in the Adaptors are needed for full activity.
Figure S10. U1 Adaptor treatment does not elicit an immune response at 4 hours.
Figure S11. U1 Adaptor treatment does not elicit an immune response at 24 hours.

Acknowledgments. This work was done in Piscataway, New Jersey; Hillsborough, New Jersey; and Coralville, Iowa. This work was supported by the National Institutes of Health SBIR grants R43CA153842 to R.G. and S.C. and 5R44GM085863-03 to M.A.B, and an National Institute of Environmental Health Sciences center grant ES005022. This work was also supported by grants to S.I.G. and S.C. from the QED Proof-of-Concept Program (University City Science Center) and the Busch Biomedical Research Program. We also thank the Rutgers University Summer Undergraduate Research Fellowship (SURF) fellowship program and Aresty Center for supporting the undergraduate research performed by N.H.Z., C.J., N.R.P., S.Z., C.M., and S.A.S. We thank members of the Gunderson and Chen labs, the Rutgers University/University of Medicine and Dentistry New Jersey RNA community, the IDT Molecular Genetics & Biophysics group for advice and comments during the course of this work and Li Gu of the Kathryn Uhrich lab for instructing us on use of their Malvern Zetasizer instrument. S.I.G. and R.G. declare competing financial interests due to part ownership of Silagene Inc. M.A.B. and K.A.L. are employed by Integrated DNA Technologies, Inc., (IDT) which offers oligonucleotides for sale similar to some of the compounds described in the manuscript. IDT is, however, not a publicly traded company and neither author personally owns any shares/equity in IDT. The other authors declared no conflict of interest.

1. Elbashir, SM, Harborth, J, Lendeckel, W, Yalcin, A, Weber, K and Tuschl, T (2001). Duplexes of 21-nucleotide RNAs mediate RNA interference in cultured mammalian cells. *Nature* **411**: 494–498.
2. Castanotto, D and Rossi, JJ (2009). The promises and pitfalls of RNA-interference-based therapeutics. *Nature* **457**: 426–433.
3. Kurreck, J (2003). Antisense technologies. Improvement through novel chemical modifications. *Eur J Biochem* **270**: 1628–1644.
4. Bauman, J, Jearawiriyapaisarn, N and Kole, R (2009). Therapeutic potential of splice-switching oligonucleotides. *Oligonucleotides* **19**: 1–13.
5. Lennox, KA and Behlke, MA (2011). Chemical modification and design of anti-miRNA oligonucleotides. *Gene Ther* **18**: 1111–1120.
6. Haussecker, D (2008). The business of RNAi therapeutics. *Hum Gene Ther* **19**: 451–462.
7. Goraczniak, R, Behlke, MA and Gunderson, SI (2009). Gene silencing by synthetic U1 adaptors. *Nat Biotechnol* **27**: 257–263.
8. Roca, X and Krainer, AR (2009). A splicing component adapted to gene silencing. *Nat Biotechnol* **27**: 250–251.
9. Furth, PA, Choe, WT, Rex, JH, Byrne, JC and Baker, CC (1994). Sequences homologous to 5' splice sites are required for the inhibitory activity of papillomavirus late 3' untranslated regions. *Mol Cell Biol* **14**: 5278–5289.

10. Gunderson, SI, Polycarpou-Schwarz, M and Mattaj, IW (1998). U1 snRNP inhibits pre-mRNA polyadenylation through a direct interaction between U1 70K and poly(A) polymerase. *Mol Cell* **1**: 255–264.
11. Proudfoot, NJ, Furger, A and Dye, MJ (2002). Integrating mRNA processing with transcription. *Cell* **108**: 501–512.
12. Danckwardt, S, Hentze, MW and Kulozik, AE (2008). 3' end mRNA processing: molecular mechanisms and implications for health and disease. *EMBO J* **27**: 482–498.
13. Levin, AA (1999). A review of the issues in the pharmacokinetics and toxicology of phosphorothioate antisense oligonucleotides. *Biochim Biophys Acta* **1489**: 69–84.
14. Prakash, TP (2011). An overview of sugar-modified oligonucleotides for antisense therapeutics. *Chem Biodivers* **8**: 1616–1641.
15. Guga, P and Koziolkiewicz, M (2011). Phosphorothioate nucleotides and oligonucleotides - recent progress in synthesis and application. *Chem Biodivers* **8**: 1642–1681.
16. Yoo, BH, Bochkareva, E, Bochkarev, A, Mou, TC and Gray, DM (2004). 2'-O-methyl-modified phosphorothioate antisense oligonucleotides have reduced non-specific effects in vitro. *Nucleic Acids Res* **32**: 2008–2016.
17. Behlke, MA (2008). Chemical modification of siRNAs for in vivo use. *Oligonucleotides* **18**: 305–319.
18. Vickers, TA, Sabripour, M and Crooke, ST (2011). U1 adaptors result in reduction of multiple pre-mRNA species principally by sequestering U1snRNP. *Nucleic Acids Res* **39**: e71.
19. McGill, GG, Horstmann, M, Widlund, HR, Du, J, Motyckova, G, Nishimura, EK *et al.* (2002). Bcl2 regulation by the melanocyte master regulator Mitf modulates lineage survival and melanoma cell viability. *Cell* **109**: 707–718.
20. Zhao, H, Peng, P, Longley, C, Zhang, Y, Borowski, V, Mehlig, M *et al.* (2007). Delivery of G3139 using releasable PEG-linkers: impact on pharmacokinetic profile and anti-tumor efficacy. *J Control Release* **119**: 143–152.
21. Loriot, Y, Mordant, P, Brown, BD, Bourhis, J, Soria, JC and Deutsch, E (2010). Inhibition of BCL-2 in small cell lung cancer cell lines with oblimersen, an antisense BCL-2 oligodeoxynucleotide (ODN): in vitro and in vivo enhancement of radiation response. *Anticancer Res* **30**: 3869–3878.
22. Ocker, M, Neureiter, D, Lueders, M, Zopf, S, Ganslmayer, M, Hahn, EG *et al.* (2005). Variants of bcl-2 specific siRNA for silencing antiapoptotic bcl-2 in pancreatic cancer. *Gut* **54**: 1298–1308.
23. Okamoto, K, Ocker, M, Neureiter, D, Dietze, O, Zopf, S, Hahn, EG *et al.* (2007). bcl-2-specific siRNAs restore gemcitabine sensitivity in human pancreatic cancer cells. *J Cell Mol Med* **11**: 349–361.
24. Jansen, B, Wacheck, V, Heere-Ress, E, Schlagbauer-Wadl, H, Hoeller, C, Lucas, T *et al.* (2000). Chemosensitisation of malignant melanoma by BCL2 antisense therapy. *Lancet* **356**: 1728–1733.
25. Yip, KW and Reed, JC (2008). Bcl-2 family proteins and cancer. *Oncogene* **27**: 6398–6406.
26. Gross, A, McDonnell, JM and Korsmeyer, SJ (1999). BCL-2 family members and the mitochondria in apoptosis. *Genes Dev* **13**: 1899–1911.
27. Jansen, B, Schlagbauer-Wadl, H, Brown, BD, Bryan, RN, van Elsas, A, Müller, M et al. (1998). bcl-2 antisense therapy chemosensitizes human melanoma in SCID mice. *Nat Med* **4**: 232–234.
28. Danial, NN and Korsmeyer, SJ (2004). Cell death: critical control points. *Cell* **116**: 205–219.
29. Miller, AJ and Mihm, MC Jr (2006). Melanoma. *N Engl J Med* **355**: 51–65.
30. Yip, D, Le, MN, Chan, JL, Lee, JH, Mehnert, JA, Yudd, A *et al.* (2009). A phase 0 trial of riluzole in patients with resectable stage III and IV melanoma. *Clin Cancer Res* **15**: 3896–3902.
31. Pollock, PM, Cohen-Solal, K, Sood, R, Namkoong, J, Martino, JJ, Koganti, A *et al.* (2003). Melanoma mouse model implicates metabotropic glutamate signaling in melanocytic neoplasia. *Nat Genet* **34**: 108–112.
32. Lee, HJ, Wall, B and Chen, S (2008). G-protein-coupled receptors and melanoma. *Pigment Cell Melanoma Res* **21**: 415–428.
33. Speyer, CL, Smith, JS, Banda, M, DeVries, JA, Mekani, T and Gorski, DH (2012). Metabotropic glutamate receptor-1: a potential therapeutic target for the treatment of breast cancer. *Breast Cancer Res Treat* **132**: 565–573.
34. Rettig, GR and Behlke, MA (2012). Progress toward in vivo use of siRNAs-II. *Mol Ther* **20**: 483–512.
35. Zitzmann, S, Ehemann, V and Schwab, M (2002). Arginine-glycine-aspartic acid (RGD)-peptide binds to both tumor and tumor-endothelial cells in vivo. *Cancer Res* **62**: 5139–5143.
36. Temming, K, Meyer, DL, Zabinski, R, Dijkers, EC, Poelstra, K, Molema, G *et al.* (2006). Evaluation of RGD-targeted albumin carriers for specific delivery of auristatin E to tumor blood vessels. *Bioconjug Chem* **17**: 1385–1394.
37. Wolinsky, JB and Grinstaff, MW (2008). Therapeutic and diagnostic applications of dendrimers for cancer treatment. *Adv Drug Deliv Rev* **60**: 1037–1055.
38. Kaminskas, LM, Boyd, BJ and Porter, CJ (2011). Dendrimer pharmacokinetics: the effect of size, structure and surface characteristics on ADME properties. *Nanomedicine (Lond)* **6**: 1063–1084.
39. Cheng, Y, Wang, J, Rao, T, He, X and Xu, T (2008). Pharmaceutical applications of dendrimers: promising nanocarriers for drug delivery. *Front Biosci* **13**: 1447–1471.
40. Myc, A, Kukowska-Latallo, J, Cao, P, Swanson, B, Battista, J, Dunham, T *et al.* (2010). Targeting the efficacy of a dendrimer-based nanotherapeutic in heterogeneous xenograft tumors in vivo. *Anticancer Drugs* **21**: 186–192.
41. Davis, ME (2009). The first targeted delivery of siRNA in humans via a self-assembling, cyclodextrin polymer-based nanoparticle: from concept to clinic. *Mol Pharm* **6**: 659–668.
42. Alam, MR, Dixit, V, Kang, H, Li, ZB, Chen, X, Trejo, J *et al.* (2008). Intracellular delivery of an anionic antisense oligonucleotide via receptor-mediated endocytosis. *Nucleic Acids Res* **36**: 2764–2776.
43. Juliano, R, Alam, MR, Dixit, V and Kang, H (2008). Mechanisms and strategies for effective delivery of antisense and siRNA oligonucleotides. *Nucleic Acids Res* **36**: 4158–4171.
44. Davies, H, Bignell, GR, Cox, C, Stephens, P, Edkins, S, Clegg, S *et al.* (2002). Mutations of the BRAF gene in human cancer. *Nature* **417**: 949–954.
45. Pollock, PM, Harper, UL, Hansen, KS, Yudt, LM, Stark, M, Robbins, CM *et al.* (2003). High frequency of BRAF mutations in nevi. *Nat Genet* **33**: 19–20.
46. Shin, SS, Namkoong, J, Wall, BA, Gleason, R, Lee, HJ and Chen, S (2008). Oncogenic activities of metabotropic glutamate receptor 1 (Grm1) in melanocyte transformation. *Pigment Cell Melanoma Res* **21**: 368–378.
47. Lee, HJ, Wall, BA, Wangari-Talbot, J, Shin, SS, Rosenberg, S, Chan, JL *et al.* (2011). Glutamatergic pathway targeting in melanoma: single-agent and combinatorial therapies. *Clin Cancer Res* **17**: 7080–7092.
48. Robbins, M, Judge, A, Ambegia, E, Choi, C, Yaworski, E, Palmer, L *et al.* (2008). Misinterpreting the therapeutic effects of small interfering RNA caused by immune stimulation. *Hum Gene Ther* **19**: 991–999.
49. Robbins, M, Judge, A and MacLachlan, I (2009). siRNA and innate immunity. *Oligonucleotides* **19**: 89–102.
50. Krieg, AM (2006). Therapeutic potential of Toll-like receptor 9 activation. *Nat Rev Drug Discov* **5**: 471–484.
51. Fujimoto, C, Nakagawa, Y, Ohara, K and Takahashi, H (2004). Polyriboinosinic polyribocytidylic acid [poly(I:C)]/TLR3 signaling allows class I processing of exogenous protein and induction of HIV-specific CD8+ cytotoxic T lymphocytes. *Int Immunol* **16**: 55–63.
52. Semple, SC, Akinc, A, Chen, J, Sandhu, AP, Mui, BL, Cho, CK *et al.* (2010). Rational design of cationic lipids for siRNA delivery. *Nat Biotechnol* **28**: 172–176.
53. Love, KT, Mahon, KP, Levins, CG, Whitehead, KA, Querbes, W, Dorkin, JR *et al.* (2010). Lipid-like materials for low-dose, in vivo gene silencing. *Proc Natl Acad Sci USA* **107**: 1864–1869.
54. Zhou, J, Neff, CP, Liu, X, Zhang, J, Li, H, Smith, DD *et al.* (2011). Systemic administration of combinatorial dsiRNAs via nanoparticles efficiently suppresses HIV-1 infection in humanized mice. *Mol Ther* **19**: 2228–2238.
55. Poeck, H, Besch, R, Maihoefer, C, Renn, M, Tormo, D, Morskaya, SS *et al.* (2008). 5'-Triphosphate-siRNA: turning gene silencing and Rig-I activation against melanoma. *Nat Med* **14**: 1256–1263.
56. Manzoni, L, Belvisi, L, Arosio, D, Bartolomeo, MP, Bianchi, A, Brioschi, C *et al.* (2012). Synthesis of Gd and (68)Ga complexes in conjugation with a conformationally optimized RGD sequence as potential MRI and PET tumor-imaging probes. *ChemMedChem* **7**: 1084–1093.
57. Castanotto, D, Sakurai, K, Lingeman, R, Li, H, Shively, L, Aagaard, L *et al.* (2007). Combinatorial delivery of small interfering RNAs reduces RNAi efficacy by selective incorporation into RISC. *Nucleic Acids Res* **35**: 5154–5164.
58. Vickers, TA, Lima, WF, Nichols, JG and Crooke, ST (2007). Reduced levels of Ago2 expression result in increased siRNA competition in mammalian cells. *Nucleic Acids Res* **35**: 6598–6610.
59. Wu, TY, Saw, CL, Khor, TO, Pung, D, Boyanapalli, SS and Kong, AN (2012). In vivo pharmacodynamics of indole-3-carbinol in the inhibition of prostate cancer in transgenic adenocarcinoma of mouse prostate (TRAMP) mice: involvement of Nrf2 and cell cycle/apoptosis signaling pathways. *Mol Carcinog* **51**: 761–770.

Supplementary Information accompanies this paper on the Molecular Therapy–Nucleic Acids website (http://www.nature.com/mtna)